Original Article

DOI: 10.5582/bst.2017.01267

Low-density lipoprotein receptor deficiency impaired mice osteoblastogenesis *in vitro*

Na Zhang[1,2,3,§], Yang Zhang[4,§], Jing Lin[1,2,3], Xuemin Qiu[1,2,3], Lanting Chen[1,2,3], Xinyao Pan[1,2,3], Youhui Lu[1,2,3], Jiali Zhang[1,2,3], Yan Wang[1,2,3], Dajin Li[1,2,3], Ling Wang[1,2,3,*]

[1] *Hospital & Institute of Obstetrics and Gynecology, Fudan University, Shanghai, China;*
[2] *The Academy of Integrative Medicine of Fudan University, Shanghai, China;*
[3] *Shanghai Key Laboratory of Female Reproductive Endocrine Related Diseases, Shanghai, China;*
[4] *First Affiliated Hospital, Heilongjiang University of Chinese Medicine, Harbin, China.*

Summary **Postmenopausal osteoporosis affected most elderly women with co-existence of lipid and bone metabolism disorders. However, the cellular and molecular mechanisms underlying the parallel progression and cross-talk of these systems remained unclear. In the present study, low-density lipoprotein receptor knockout (*LDLR*$^{-/-}$) mice were chosen to elucidate the effect of LDLR in regulating the differentiation of osteoblasts, which were responsible for bone formation and modulation of osteoclastogenesis. Primary osteoblasts were isolated from the calvarium of newborn *LDLR*$^{-/-}$ or wild-type mice followed by osteoblastic differentiation culture *in vitro*. Alkaline phosphatase activity was significantly decreased in *LDLR*$^{-/-}$ osteoblasts compared to wild-type controls, combined with calcium deposit formation delay, implying impaired osteoblastogenesis *in vitro*. Consistent with these findings, the expression of *runt-related transcription factor 2* (*Runx2*) was decreased 3 days after differentiation in *LDLR*$^{-/-}$ osteoblasts compared to wild-type controls. Moreover, the expression of *Osterix* was decreased 7 days after differentiation in *LDLR*$^{-/-}$ osteoblasts compared to wild-type controls, later than Runx2. However, the osteoclastogenesis modulation role of osteoblasts was unaffected by the LDLR deficiency, evidenced by the same level of osteoprotegerin (OPG)/receptor activator of nuclear factor-κ B ligand (RANKL) axis between *LDLR*$^{-/-}$ and wild-type control osteoblasts. Our results provide a novel insight into the role of LDLR during osteoblastic differentiation and improve understanding of cross-talk between bone and lipid metabolisms.**

Keywords: Postmenopausal osteoporosis, low-density lipoprotein receptor, osteoblast, osteoblastogenesis, alkaline phosphatase, runt-related transcription factor 2, Osterix

1. Introduction

Postmenopausal osteoporosis (PMO) affected most elderly women due to estrogen decline. Several epidemiological studies demonstrated the co-existence of lipid and bone metabolism disorders in postmenopausal females (*1-3*). Recent studies indicated a positive connection between cardiovascular disease and risk of osteoporosis, because high cholesterol levels and high low-density lipoprotein (LDL)-cholesterol levels had been described to correlate with low bone mineral density in PMO patients (*4-7*). Furthermore, the increased serum LDL-cholesterol level was indicated to be an index affecting the presence of prevalent non-vertebral fractures in postmenopausal females (*8*). Additionally, menopausal hormone therapy exerted benefit effects of reducing the risk of atherosclerosis (*9-11*). Therefore, hyperlipidemia may play an essential role in regulating osteoporosis progress.

Osteoporosis, a systemic metabolic skeletal disorder characterized by low bone mass and increased risk of fractures, is a consequence of bone turnover disruption caused by imbalance between osteoblast-mediated bone formation and osteoclast-mediated bone resorption. Pre-

Released online in J-STAGE as advance publication December 19, 2017.

[§]These authors contributed equally to this work.

**Address correspondence to:*
Dr. Ling Wang, Obstetrics & Gynecology Hospital of Fudan University, 413 Zhaozhou Road, Shanghai, 200011, China.
E-mail: Dr.wangling@fudan.edu.cn

osteoblasts were derived from pluripotent mesenchymal stem cells (MSCs), which were also the progenitors of adipocytes and chondrocytes (*12*). Osteoblastogenesis could be defined by four sequential stages: lineage commitment, proliferation, extracellular matrix (ECM) synthesis, and matrix mineralization (*13*). Runt-related transcription factor 2 (Runx2) was the master transcription regulator of osteoblast lineage commitment that inhibited MSCs from differentiating into the adipocytic lineages (*14*). Null mutation of *Runx2* in mice resulted in a cartilaginous skeleton with complete lack of osteoblasts (*15-17*). Runx2 regulated osteoblast-related molecules such as Osterix, type I collagen and alkaline phosphatase (ALP). Osterix was the second transcription factor for proliferative expansion of immature osteoblasts, and the expression of *Osterix* was absent in *Runx2* null mice but *Runx2* was expressed in *Osterix* null mice (*18,19*). Type I collagen was one of the major osteoblast-specific matrix proteins expressed by fully differentiated osteoblasts after complete mitosis, essential for both bone matrix synthesis and later mineralization (*20,21*). Moreover, osteoblasts took part in the regulation of osteoclastogenesis and bone resorption by producing receptor activator of nuclear factor-κ B ligand (RANKL), the ligand of RANK present in osteoclast precursor cells, and its decoy receptor osteoprotegerin (OPG) (*22*). Precise regulation of osteoblastogenesis and osteoclastogenesis was required for the maintenance of normal bone metabolism.

Several basic studies had established that oxidized-LDL inhibited osteoblastic differentiation and promoted adipocytic differentiation of MSCs *in vitro* (*23,24*). Moreover, oxidized-LDL increased *RANKL* expression and secretion in human osteoblast-like cells (*24-26*), indicating cross-talk between lipid and bone metabolism systems. LDL was transferred in particle form and internalized by binding to the receptor LDL receptor (LDLR) residing on the surface of liver cells (*27*). LDLR was the prototype member of the LDLR family that contained several key regulators involved in osteoblastic development. For example, human osteoblasts expressed low-density lipoprotein receptor-related protein (LRP) 1 with a capacity for osteocalcin carboxylation (*28*). LRP4, LRP5/6, and LRP8 were involved in the maintenance of bone (*29-36*). However, the role of LDLR in bone metabolism was unclear with controversial results in recent studies. LDLR deficient familial hypercholesterolemia patients showed normal bone mineral density at the femora neck (*37*). In an animal experiment, LDLR deficiency caused ectopic bone formation in an experimental osteoarthritis mouse model (*38*). Furthermore, Okayasu *et al*. showed that LDLR deficiency induced impaired pre-osteoclast fusion *in vitro* while increasing bone mass in LDLR deficient mice (*39*). However, decreased bone mass was detected in LDLR deficient mice with inhibition of osteoblastogenesis from bone marrow cells and enhanced osteoclastogenesis *in vitro* (*40*), indicating that LDLR might regulate bone metabolism in a complex manner.

Previous work from our group showed that most of the LDLR family members were up-regulated during osteoblastic differentiation *in vitro*, except for LDLR, which was down-regulated in the late stages of pre-osteoblast mineralization culture, indicating a unique role of LDLR in osteoblastogenesis (*41*). The function of LDLR in regulating osteoblastic development and related mechanisms remained to be further explored. In the present study, we made use of LDLR deficient mice and pre-osteoblasts *in vitro* culture system to explore the effect of LDLR deficiency on this process.

2. Materials and Methods

2.1. *Mice*

LDLR knockout (*LDLR*$^{-/-}$) mouse strain (B6.129S7-Ldlrtm1Her/J) was purchased from Nanjing Biomedical Research Institute of Nanjing University (Nanjing, China), originally from the Jackson Laboratory. Data obtained from C57BL/6 wild-type (WT) mice purchased from the Laboratory Animal Facility of Chinese Academy of Science (Shanghai, China) were used as controls. After being habituated to housing conditions for 3 days, mice were mated (one male with two females per cage) under standard housing conditions at 24°C on a reversed 12-12 hour light-dark cycle. Standard rodent food and water were provided ad libitum at room temperature. Primary osteoblasts were isolated from the calvarium of newborn mice. Experimental animal housing and handling were conducted in accordance with guidelines for the care and use of laboratory animals at Fudan University, Shanghai, China and in conformity with the National Institutes of Health Guide for Care and Use of Laboratory Animals (Publication No. 85-23, revised 1985).

2.2. *Chemicals and reagents*

Serum and phenol red-free minimal essential medium (α-MEM) and fetal bovine serum (FBS) were purchased from Gibco-BRL (Gaithersburg, MD, USA). Dexamethasone, β-glycerophosphate disodium salt hydrate, ascorbic acid, and collagenase were obtained from Sigma-Aldrich Co (Saint Louis, MO, USA). Dispase was supplied by Hoffmann-La Roche Ltd (Basel, Schweiz). RNAiso Plus, PrimeScriptTM RT Master Mix (Perfect Real Time) Kit and SYBR Premix Ex Taq II (Tli RNaseH Plus) Kit were obtained from TaKaRa biotechnology (Otsu, Japan). 2×GC rich PCR MasterMix was purchased from Tiangen Biotech (Beijing) Co., Ltd (Beijing, China). BCIP/NBT Alkaline Phosphatase Color Development Kit, Alkaline Phosphatase Assay Kit and penicillin-streptomycin were obtained from the Beyotime

Institute of Biotechnology (Shanghai, China). Alizarin Staining kit was supplied by Genmed (Shanghai, China). All primers were synthesized by Shanghai Shenggong Company (Shanghai, China).

2.3. *Genomic DNA isolation and genotyping*

Genotypes of *LDLR*$^{-/-}$ mice were confirmed by polymerase chain reaction (PCR) analyses of genomic DNA. Generally, tissue samples were collected and incubated in 50mM NaOH at 95°C for 15 min. Then 1/10 of total volume 1M Tris HCl (PH = 8.0) was added and mixed well. After centrifugation at 12,000g for 15 min at room temperature, the supernatant was used for further PCR analyses with 2×GC rich PCR MasterMix. Touchdown PCR reaction was performed using the following conditions according to the protocol from the Jackson Laboratory website: 94°C for 2 min, followed by 10 cycles of 94°C for 20 sec, annealing temperature for 15 sec decreased 0.5°C every second cycle from 65°C, 68°C for 10 sec, then another 28 cycles of 94°C for 15 sec, 60°C for 15 sec, and 72°C for 10 sec, and finally an additional step of 72°C for 2 min before the end of the program. Primer mixture was made of 3 primers and the sequences are listed in Table 1. PCR product was electrophoresed on 1.5% low melting point agarose gel. The homozygote mutant showed a product of 179bp length with 351 bp for wild-type. The heterozygote mutant showed two separated bands of 179bp and 351bp length (Figure 1).

Table 1. Summary of oligonucleotide primers for *LDLR*$^{-/-}$ mice genotyping

Oligonucleotide	Sequence* (5'-3')
Common forward primer	TATGCATCCCCAGTCTTTGG
Wild-type reverse primer	CTACCCAACCAGCCCCTTAC
Mutant reverse primer	ATAGATTCGCCCTTGTGTCC

*The oligonucleotide sequences for genotyping were obtained from the Jackson Laboratory website: *https://www.jax.org/search?q=+002207*

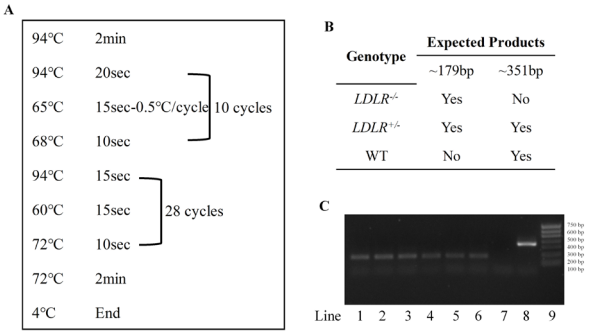

Figure 1. Schematic diagrams for the genotyping of the *LDLR*$^{-/-}$ mouse strain. Genomic DNA was isolated from the tissue samples and further analyzed by touchdown PCR reaction with primer mixture containing three primers. **(A)** The program cycle for touchdown PCR reaction. **(B)** Expected results for each mouse strain. **(C)** Gel image for the PCR products of *LDLR*$^{-/-}$ and wild-type (WT) mice, while ddH20 was served as the blank control. Line1-6: *LDLR*$^{-/-}$ mice with a product of ~179 bp, Line 7: ddH2O, Line 8: WT mice with a product of ~351 bp and Line 9: DNA marker. bp: base pair.

2.4. *Primary osteoblasts isolation*

Primary osteoblasts isolated from the calvarium of newborn mice were separated two days before the Osteogenic Induction Media treatment as described previously (*41*). Briefly, skull bones were extracted and digested in α-MEM medium with 0.1% collagenase and 0.2% dispase for 10 min at 94°C vortexed at 180 rpm, and the supernatant was discarded, then the digestion treatment was repeated 4 more times. Cells from the second to fifth digestion fraction were collected and resuspended in Growth Medium, which were supplemented with 10% serum, 10 units/mL penicillin and 10 μg/mL streptomycin in α-MEM medium without phenol red. 1×10^5 cells were sowed into each well of 6-well cell culture plates and 1×10^4 into 24-well cell culture plates. The isolated primary osteoblasts were cultured in an incubator at 37°C and 5% CO_2 for 2 days until 80% confluence.

2.5. *Osteoblastic mineralization culture*

Mineralization of osteoblasts is the process during which differentiated osteoblasts are induced to produce extracellular calcium deposits *in vitro*. In the osteoblastic mineralization culture system, primary osteoblasts were treated with Osteogenic Induction Media containing 10% serum, 20 mM ascorbic acid, 1M β-glycerophosphate disodium salt hydrate, and 1 mM dexamethasone in phenol red-free α-MEM at 37°C and 5% CO_2, after reaching 80% confluence cultured in Growth Medium (*42*). Medium was refreshed once every two days. The differentiated osteoblasts were analyzed at specific time points in the following experiments.

2.6. *RNA isolation and quantitative real-time PCR*

Total RNA was isolated from primary osteoblasts in 6-well cell culture plates using the RNAiso Plus according to the manufacturer's instruction at specific time points after Osteogenic Induction Media treatment. Briefly, media was removed and 1 mL of RNAiso Plus was added into the well to lyse the cells. After homogenization by pipetting up and down, 0.2 mL chloroform per 1mL of RNAiso Plus was added to the mixture and mixed thoroughly. After incubation at room temperature for 15 min, the mixture was centrifuged for 15 min at 12,000 g at 4°C. The upper aqueous phase containing RNA was transferred to a clean tube carefully and precipitated by adding an equal volume 100% isopropanol. The RNA was concentrated by centrifugation at 12,000 g at 4°C for 10 min and washed with 75% ethanol. Then the RNA pellet was air-dried

Table 2. Summary of oligonucleotide primers for cDNA amplification

Oligonucleotide	Sequence (5'-3')
β-actin forward primer	CCTCTATGCCAACACAGT
β-actin reverse primer	AGCCACCAATCCACACAG
Col1a1 forward primer	TGACTGGAAGAGCGGAGAGTA
Col1a1 reverse primer	GACGGCTGAGTAGGGAACAC
OPG forward primer	CCTTGCCCTGACCACTCTTAT
OPG reverse primer	CGCCCTTCCTCACACTCAC
Osx forward primer	GCTCGTAGATTTCTATCCTC
Ostx reverse primer	CTTAGTGACTGCCTAACAGA
RANKL forward primer	CAAGATGGCTTCTATTACCTGT
RANKL reverse primer	TTGATGCTGGTTTTAACGAC
Runx2 forward primer	GACAGTCCCAACTTCCTGTG
Runx2 reverse primer	GCGGAGTAGTTCTCATCATTC

Col1a1: collagen type I alpha 1; OPG: osteoprotegerin; Osx: Osterix; RANKL: receptor activator of nuclear factor-κ B ligand; Runx2: runt-related transcription factor 2

for 5 min at room temperature and dissolved in RNase-free water. The reverse transcription reaction was conducted immediately after RNA isolation in a final volume of 10 μL containing 500 ng RNA sample, and 2 μL 5×PrimeScriptTM RT Master Mix (Perfect Real Time) according to the protocol from the reagent kit. Afterwards, quantitative real-time PCR was performed in a 20 μL mixture of 2 μL reverse transcription product, 10 μL 2×SYBR Premix Ex Taq II (Tli RNaseH Plus), 1.6 μL forward/reverse primer mixture for a final concentration of 0.4 μM and DNase free water up to the final volume. Reactions were performed using the following program: 95°C for 30 sec and cycles of 95°C for 5 sec and 60°C for 30 sec for 40 cycles, followed by a dissociation stage on Appliled BiosystemsInc 7900 HT (Waltham, MA, USA). Primers used are listed in Table 2. Gene expression was normalized to the level of house-keeping gene *β-actin* and analyzed using the standard $2^{-\Delta\Delta CT}$ method. All the experiments were repeated in triplicate.

2.7. *Alizarin Red S staining*

The deposited calcium deposits of differentiated primary osteoblasts were stained using Alizarin Red S according to the manufacturer's instructions as follows. After 7 days of Osteogenic Induction Media treatment in 24-well plates, cells were washed with 500 μL Cleaning Buffer and fixed with Fixation Buffer for 10 min at room temperature, then washed with Cleaning Buffer again. After fixation, 500 μL Alizarin Red S Staining Buffer was added to each well and the plate was incubated in the dark for 10 min at room temperature. The Staining Buffer was removed carefully when mineralized osteoblasts appeared bright orange-red while undifferentiated cells were slightly red or colorless. The plate was air-dried, and results were viewed by a HP scanner and recorded.

2.8. *ALP staining and activity analyses*

The ALP activity was greatly enhanced during osteoblastic differentiation *in vitro*. BCIP/NBT is the preferred staining substrate for ALP detection. After 7 days of Osteogenic Induction Media treatment in 24-well plates, cells were washed with 500 μL PBS and fixed with 4% paraformaldehyde for 20 min at room temperature, then washed with 500 μL PBS three times. The fixed cells were incubated in BCIP/NBT buffer mixed according to the protocol from the kit: 3 mL ALP Staining Buffer, 10 μL 300×BCIP Buffer and 20 μL 150×NBT Buffer for more than 30 min at room temperature avoiding light until the ALP positive differentiated osteoblasts appeared blue-violet. The reaction was stopped by adding excess deionized water. The results were visualized by a HP scanner and recorded. ALP activity in cell lysate was quantitated by using an Alkaline Phosphatase Assay kit according to the manufacturer's protocol. Absorbance was measured at 405 nm.

2.9. *Statistical analyses*

All values were presented as the mean ± SEM. Data differences were assessed by student's *t*-test with the aid of IBM SPSS software. A p value less than 0.05 was accepted as statistically significant. All experiments were repeated more than three times.

3. Results

3.1. *The LDLR deficiency inhibited the ALP activity in differentiated primary osteoblasts*

Data from our previous study showed that the expression of LDLR decreased during osteoblastic differentiation (*41*). To gain an insight into the role of LDLR in osteoblastic differentiation, we first examined the effect of LDLR deficiency on ALP activity of differentiated primary osteoblasts 7 days after Osteogenic Induction Media treatment. ALP staining showed that the ALP activity in *LDLR*$^{-/-}$ osteoblasts obviously decreased compared to osteoblasts from wild-type newborn mice (Figure 2A). The results demonstrated by ALP activity analyses showed that the ALP activity dramatically decreased in the *LDLR*$^{-/-}$ osteoblast cell lysate compared to wild-type controls (Figure 2B, $p < 0.001$), suggesting that LDLR might play a critical role in osteoblastic differentiation.

3.2. *The LDLR deficiency inhibited mineralization of differentiated primary osteoblasts*

To further test the effect of LDLR deficiency on mineralized matrix formation in osteoblasts, Alizarin Red S (ARS) staining was performed 7 days after Osteogenic Induction Media treatment. As shown in Figure 3A, calcium deposit formation labeled by ARS staining was impaired by LDLR deficiency. A marked difference in

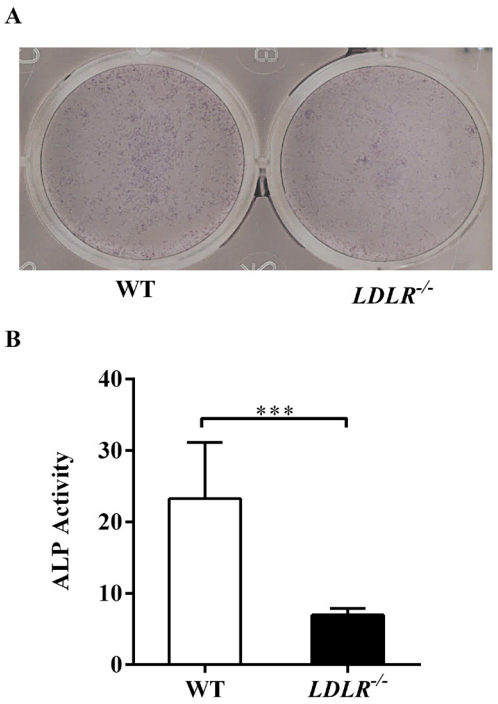

Figure 2. Impaired alkaline phosphatase (ALP) activity in the LDLR deficiency osteoblasts during differentiation *in vitro*. Primary osteoblasts from *LDLR*$^{-/-}$ or wild-type (WT) mice were treated with Osteogenic Induction Media for 7 days, respectively. Then the ALP level and activity were examined. **(A)** ALP staining showed reduced osteoblastic differentiation in *LDLR*$^{-/-}$ mice compared to WT controls. **(B)** ALP activity in the cell lysate significantly decreased in *LDLR*$^{-/-}$ osteoblasts compared to WT controls. ***$p < 0.001$.

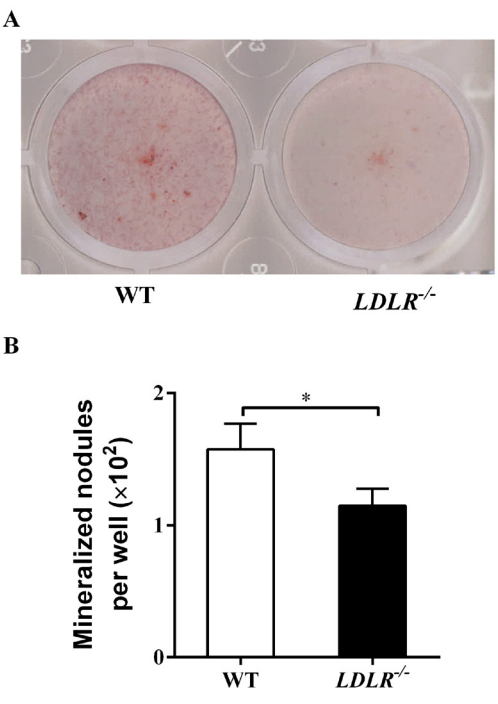

Figure 3. LDLR deficient osteoblasts showed delayed mineralization *in vitro*. After treatment with Osteogenic Induction Media for 7 days, the formation of calcium deposits was labeled using Alizarin Red S (ARS) staining of primary osteoblasts isolated from *LDLR*$^{-/-}$ or wild-type (WT) mice, respectively. **(A)** ARS staining showed reduced calcium deposit formation in *LDLR*$^{-/-}$ osteoblasts compared to WT controls. **(B)** Numbers of mineralized nodules per well were calculated from *LDLR*$^{-/-}$ or WT control osteoblasts. *$p < 0.05$.

mineralization level was also observed when comparing the number of mineralized nodules per well between the *LDLR*$^{-/-}$ and wild-type groups (Figure 3B, $p < 0.05$), indicating that LDLR might be involved in the regulation of osteoblast mineralization.

3.3. *The LDLR deficiency decreased Runx2 and Osterix expression in differentiated primary osteoblasts*

All the results above showed a potential role of LDLR in regulating osteoblastic differentiation. Runx2 was the master transcription factor and regulated a series of osteoblast-related gene expressions. We therefore inspected the mRNA level of *Runx2*. In the wild-type group, *Runx2* expression was normal at day 3 of Osteogenic Induction Media treatment and dramatically increased at day 7 compared to day 0 (Figure 4A, $p = 0.333$, $p < 0.01$). In *LDLR*$^{-/-}$ osteoblasts, *Runx2* expression decreased at day 3 of Osteogenic Induction Media treatment and increased at day 7 compared to day 0 (Figure 4A, $p < 0.05$, $p < 0.001$). When compared to the wild-type group, the *Runx2* mRNA level was slightly reduced in *LDLR*$^{-/-}$ osteoblasts at day 0, was significantly impaired at day 3, and slightly reduced again at day 7 (Figure 4A, $p = 0.488$, $p < 0.05$, $p = 0.306$), indicating LDLR might regulate osteoblastic differentiation through the effect on *Runx2* expression in the early stages of differentiation *in vitro*.

Osterix was the second key factor in osteoblastic differentiation regulated down-stream of Runx2. In the wild-type group, *Osterix* expression increased at day 3 of osteoblastic differentiation and decreased at day 7 compared to day 0 (Figure 4B, $p < 0.001$, $p < 0.001$). In *LDLR*$^{-/-}$ osteoblasts, the *Osterix* expression also significantly increased at day 3 and decreased at day 7 compared to day 0 of osteoblastic differentiation (Figure 4B, $p < 0.05$, $p < 0.01$). Compared to wild-type controls, *Osterix* expression was normal at day 3 of Osteogenic Induction Media treatment in the *LDLR*$^{-/-}$ osteoblasts, but severely decreased at day 7 (Figure 4B, $p = 0.922$, $p < 0.01$), suggesting that the effect of LDLR deficiency on Osterix might be later than Runx2 or LDLR might regulate *Osterix* expression during osteoblastic differentiation through Runx2.

We also analyzed the expression level of functional factor Collagen-1 during osteoblastic differentiation *in vitro*. *Collagen-1* expression significantly increased at day 7 of osteoblastic differentiation compared to day 0 in both *LDLR*$^{-/-}$ and wild-type groups (Figure 4C, $p < 0.001$, $p < 0.01$) and there was no significant difference at each time point between the two groups (Figure 4C, $p = 0.305$, $p = 0.243$, $p = 0.074$).

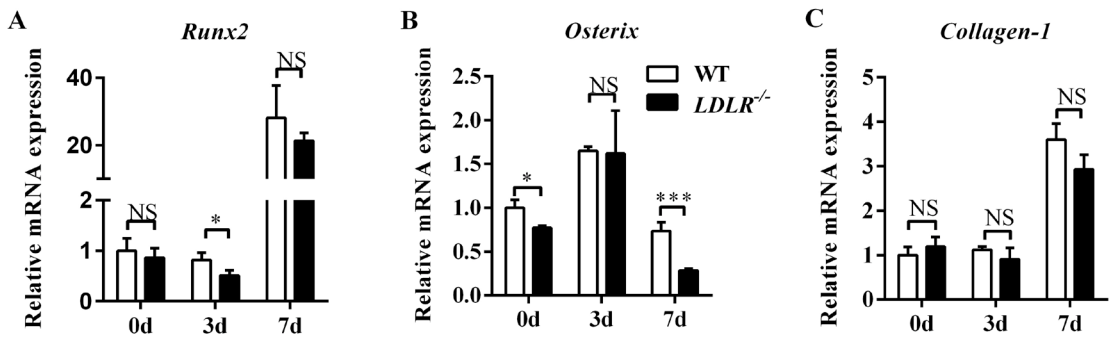

Figure 4. Relative mRNA expression levels of osteoblastic differentiation related factors. Primary osteoblasts from *LDLR*$^{-/-}$ or wild-type (WT) mice were treated with Osteogenic Induction Media for 0 day (0d), 3 days (3d) and 7 days (7d), respectively. **(A)** *Runx2*, **(B)** *Osterix* and **(C)** *Collagen-1* mRNA levels relative to that in the WT osteoblasts at day 0 of differentiation. NS, no significant difference between these groups ($P > 0.05$). *$p < 0.05$, ***$p < 0.001$.

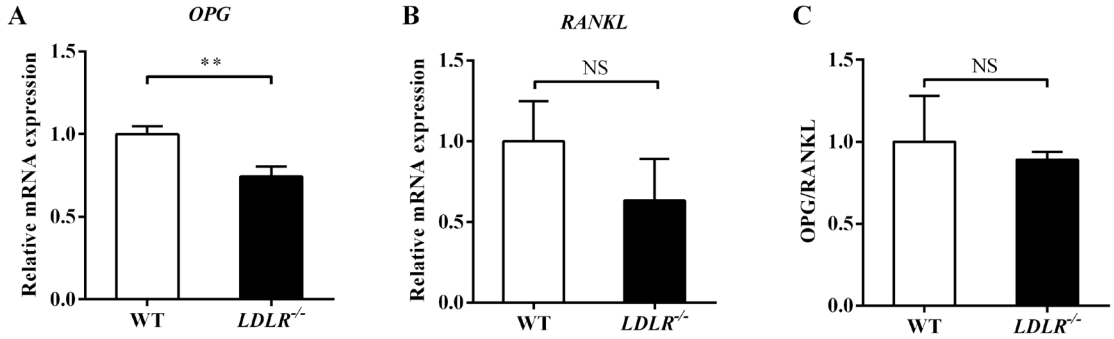

Figure 5. The OPG/RANKL level remained unaffected in LDLR deficient primary osteoblasts. Primary osteoblasts from *LDLR*$^{-/-}$ or wild-type (WT) mice were cultured in the Growth Medium until reaching 80% confluence, respectively. **(A)** *OPG* and **(B)** *RANKL* mRNA levels relative to that in the WT osteoblasts. **(C)** The ratio of *OPG/RANKL* mRNA levels relative to that in the WT osteoblasts. NS, no significant difference between these groups ($P > 0.05$). **$p < 0.01$.

3.4. *The OPG/RANKL level in osteoblast was not affected by LDLR deficiency*

Besides the bone formation role, osteoblasts could regulate osteoclastogenesis by expressing OPG and RANKL. We isolated primary osteoblasts to examine the effect of LDLR deficiency on this process. Although the expression of OPG significantly decreased in *LDLR*$^{-/-}$ osteoblasts compared to wild-type controls (Figure 5A, $p < 0.01$), the expression of RANKL was similar between the two groups (Figure 5B, $p = 0.149$). Actually, the ratio of OPG/RANKL slightly decreased in *LDLR*$^{-/-}$ osteoblasts compared to wild-type controls with no significance (Figure 5C, $p = 0.636$), suggesting that the deficiency of LDLR might have no influence on the modulation role of osteoblasts to osteoclastogenesis.

4. Discussion

Several members of the LDLR family had been shown to take part in the regulation of osteoblastogenesis. Loss-of-function mutation in LRP5 was associated with decreased bone mass in osteoporosis-pseudoglioma syndrome (OPPG; MIM259770) patients (*30*), while gain-of-function was associated with increased bone mass in other healthy patients (*43,44*). Moreover, mutation in LRP4 had been identified with high-bone-mass disorders in patients with sclerosteosis or van Buchem diseases (*33,45,46*). Our previous study showed that most of the LDLR family members increased during osteoblastic differentiation *in vitro*, such as LRP4/5/6, but the expression of LDLR decreased 25 days after differentiation *in vitro*, indicating LDLR might function in a unique way during osteoblastogenesis. To explore the effect of LDLR on osteoblastic development and function, we used a LDLR deficient mouse model and isolated pre-osteoblasts from calvarium of newborn mice. Our results showed that ALP activity of differentiated primary osteoblasts dramatically decreased in the *LDLR*$^{-/-}$ group compared to wild-type controls. The mineralization level was also impaired in the *LDLR*$^{-/-}$ group. By analyzing the expression of key transcriptional factors during osteoblastic differentiation, we confirmed that the expression of *Runx2* decreased, followed by impaired expression of *Osterix*, the direct factor regulated down-stream of Runx2, in the *LDLR*$^{-/-}$ group compared to wild-type controls. Our current study indicated that

LDLR might affect the differentiation and function of osteoblasts.

Osteoblasts originate from MSCs, which are also progenitors of adipocytes and chondrocytes. The Wnt signaling pathway played an essential role during development of osteoblasts. Activation of the Wnt signaling pathway promoted osteoblastic differentiation and inhibited expression of *peroxisome proliferator-activated receptor*-(*PPAR*-)γ. PPAR-γ was commonly considered as the key regulator of adipogenesis, and absence of PPAR-γ caused adipogenesis depletion. LRP5/LRP6 affected osteoblastogenesis by inducing the Wnt signal as co-receptor in the dual receptor complex with frizzled (FZD) (*32*). LRP4, the third member of the LRP5 and LRP6 subfamily of LDLRs, inhibited the Wnt signaling pathway by facilitating sclerostin action, the antagonist of Wnt signaling pathway (*29,36*). Dimerization of LRP6 through its LDLR domain induced canonical Wnt pathway activation (*47*). LDLR may induce the Wnt signal through the LDLR domain as well. Moreover, LRP6 could regulate LDLR-mediated LDL uptake (*48*). Is it possible that LDLR could affect the LRP6-mediated Wnt signaling pathway activation in turn? More experiments should be conducted to explore the Wnt signaling pathway activity and PPAR-γ level in the LDLR deficient osteoblasts *in vitro* and *in vivo*. The potential that LDLR deficiency might promote development of adipocytes should be further explored.

There had been controversial results in recent studies regarding the role of LDLR in bone metabolism. Okayasu *et al*. cultured bone marrow cells from *LDLR*$^{-/-}$ mice and detected reduced osteoclast formation from bone marrow cells *in vitro* with increased bone mass in these mice compared with wild-type controls. These authors attributed the reduction in osteoclast formation to a defect in cell-cell fusion of preosteoclasts. Furthermore, these authors demonstrated that the *LDLR*$^{-/-}$ derived preosteoclasts contained less osteoclast fusion regulator molecules such as Atp6v0d2 and DC-STAMP in the plasma membrane than those from wild-type preosteoclasts (*39*). However, Chen and colleagues detected decreased bone mass in the *LDLR*$^{-/-}$ mice, which was associated with decreased *Runx2* and *Collangen-1* expression during osteoblastogenesis and increased TRAP levels during osteoclastogenesis from bone marrow cells *in vitro*, implying that the decreased bone mass in *LDLR*$^{-/-}$ mice was associated with decreased osteoblastic function and increased osteoclastic function in these mice (*40*). In the present study, we isolated pre-osteoblasts from the calvarium of newborn *LDLR*$^{-/-}$ mice and detected ALP activity, calcium deposit formation, and osteoblastogenesis related factor expression 0, 3, and 7 days after differentiation. The activity of ALP decreased in *LDLR*$^{-/-}$ osteoblasts 7 days after differentiation compared to wild-type controls, combined with impaired calcium deposit formation that indicated inhibited mineralization of differentiated osteoblasts. Consistent with impaired osteoblastogenesis, the expression of *Runx2* decreased 3 days after differentiation of *LDLR*$^{-/-}$ osteoblasts compared to wild-type controls, followed by decreased *Osterix* expression 7 days after differentiation, implying that LDLR might regulate *Osterix* expression during osteoblastic differentiation through Runx2. However, the modulation role of osteoblasts on osteoclastogenesis was not affected by LDLR deficiency, evidenced by the same level of the OPG/RANKL ratio between *LDLR*$^{-/-}$ and wild-type control osteoblasts. The bone mass and bone microarchitecture of *LDLR*$^{-/-}$ and wild-type mice *in vivo* should be analyzed in further studies.

The specific function of LDLR was to remove LDL-cholesterol particles from the circulation (*49,50*). Once entering endosomes, the LDL-LDLR complex dissociated due to the local low PH and the receptor was recycled to the plasma membrane for clearance of more cholesterol and cholesterol ester-containing LDL particles from the circulation. Then LDL was transported to lysosomes and degraded (*51*), Moreover, the degradation of LDLR was mediated by binding to proprotein convertase subtilisin/kexin type 9 (PCSK9). Interestingly, 17α-ethinyl estradiol treatment increased the binding of LDL to liver cell membranes *in vitro*. Moreover, the removal rate of rat and human LDL from blood plasma increased in estrogen-treated rats (*52,53*). Additionally, 17α-ethinyl estradiol at a pharmacologic dose increased LDLR number and mRNA level in livers of rabbits (*54*). In pituitary GH3 somatolactotropes, LDLR expression level and LDL uptake were up-regulated by estrogen treatment (*55*). Furthermore, the absence of PCSK9-triggered LDLR degradation led to a sex- and tissue-dependent subcellular distribution of LDLR that depends on estrogens (*56*). All the results indicated that LDLR may contribute to estrogen-mediated bone metabolism. Further studies are required to explore the effect of LDLR deficiency on ovariectomy-induced bone loss and its corresponding bone metabolism changes.

In conclusion, osteoblastic differentiation was disrupted by LDLR deficiency *in vitro*. Alkaline phosphatase activity significantly decreased in *LDLR*$^{-/-}$ osteoblasts *in vitro* compared to wild-type controls, combined with calcium deposit formation delay. LDLR deficiency reduced the expression of *Runx2* in early stages and down-regulated *Osterix* in later stages during osteoblastic development *in vitro*, but the OPG/RANKL level remained unaffected in *LDLR*$^{-/-}$ osteoblasts compared with wild-type controls *in vitro*.

Acknowledgements

This work was supported by the National Natural Science Foundation of China No. 31571196 (to Ling Wang), the Science and Technology Commission of Shanghai Municipality 2015 YIXUEYINGDAO

project No. 15401932200 (to Ling Wang), the FY2008 JSPS Postdoctoral Fellowship for Foreign Researchers P08471 (to Ling Wang), the National Natural Science Foundation of China No. 30801502 (to Ling Wang), the Shanghai Pujiang Program No. 11PJ1401900 (to Ling Wang), Development Project of Shanghai Peak Disciplines-Integrative Medicine No.20150407, and Shanghai Municipal Commission of Health and Family Planning Science Foundation for Young Scientists No. 20174Y0224 (to Na Zhang).

References

1. Banks LM, Lees B, MacSweeney JE, Stevenson JC. Effect of degenerative spinal and aortic calcification on bone density measurements in post-menopausal women: links between osteoporosis and cardiovascular disease? Eur J Clin Invest. 1994; 24:813-817.
2. Li S, Guo H, Liu Y, Wu F, Zhang H, Zhang Z, Xie Z, Sheng Z, Liao E. Relationships of serum lipid profiles and bone mineral density in postmenopausal Chinese women. Clin Endocrinol (Oxf). 2015; 82:53-58.
3. von der Recke P, Hansen MA, Hassager C. The association between low bone mass at the menopause and cardiovascular mortality. Am J Med. 1999; 106:273-278.
4. Bijelic R, Balaban J, Milicevic S. Correlation of the lipid profile, BMI and bone mineral density in postmenopausal women. Mater Sociomed. 2016; 28:412-415.
5. Cui LH, Shin MH, Chung EK, Lee YH, Kweon SS, Park KS, Choi JS. Association between bone mineral densities and serum lipid profiles of pre- and post-menopausal rural women in South Korea. Osteoporos Int. 2005; 16:1975-1981.
6. Figueiredo CP, Rajamannan NM, Lopes JB, Caparbo VF, Takayama L, Kuroishi ME, Oliveira IS, Menezes PR, Scazufca M, Bonfa E, Pereira RM. Serum phosphate and hip bone mineral density as additional factors for high vascular calcification scores in a community-dwelling: the Sao Paulo Ageing & Health Study (SPAH). Bone. 2013; 52:354-359.
7. Hofbauer LC, Brueck CC, Shanahan CM, Schoppet M, Dobnig H. Vascular calcification and osteoporosis--from clinical observation towards molecular understanding. Osteoporos Int. 2007; 18:251-259.
8. Yamauchi M, Yamaguchi T, Nawata K, Tanaka K, Takaoka S, Sugimoto T. Increased low-density lipoprotein cholesterol level is associated with non-vertebral fractures in postmenopausal women. Endocrine. 2015; 48:279-286.
9. Barrett-Connor E, Bush TL. Estrogen and coronary heart disease in women. JAMA. 1991; 265:1861-1867.
10. Stampfer MJ, Colditz GA. Estrogen replacement therapy and coronary heart disease: a quantitative assessment of the epidemiologic evidence. Prev Med. 1991; 20:47-63.
11. Terauchi M, Honjo H, Mizunuma H, Aso T. Effects of oral estradiol and levonorgestrel on cardiovascular risk markers in postmenopausal women. Arch Gynecol Obstet. 2012; 285:1647-1656.
12. Chamberlain G, Fox J, Ashton B, Middleton J. Concise review: mesenchymal stem cells: their phenotype, differentiation capacity, immunological features, and potential for homing. Stem Cells. 2007; 25:2739-2749.
13. Titorencu I, Pruna V, Jinga VV, Simionescu M. Osteoblast ontogeny and implications for bone pathology: an overview. Cell Tissue Res. 2014; 355:23-33.
14. Komori T. Regulation of osteoblast differentiation by transcription factors. J Cell Biochem. 2006; 99:1233-1239.
15. Ducy P, Zhang R, Geoffroy V, Ridall AL, Karsenty G. Osf2/Cbfa1: a transcriptional activator of osteoblast differentiation. Cell. 1997; 89:747-754.
16. Komori T, Yagi H, Nomura S, et al. Targeted disruption of Cbfa1 results in a complete lack of bone formation owing to maturational arrest of osteoblasts. Cell. 1997; 89:755-764.
17. Otto F, Thornell AP, Crompton T, Denzel A, Gilmour KC, Rosewell IR, Stamp GW, Beddington RS, Mundlos S, Olsen BR, Selby PB, Owen MJ. Cbfa1, a candidate gene for cleidocranial dysplasia syndrome, is essential for osteoblast differentiation and bone development. Cell. 1997; 89:765-771.
18. Nakashima K, Zhou X, Kunkel G, Zhang Z, Deng JM, Behringer RR, de Crombrugghe B. The novel zinc finger-containing transcription factor osterix is required for osteoblast differentiation and bone formation. Cell. 2002; 108:17-29.
19. Zhang C. Transcriptional regulation of bone formation by the osteoblast-specific transcription factor Osx. J Orthop Surg Res. 2010; 5:37.
20. Murshed M, Harmey D, Millan JL, McKee MD, Karsenty G. Unique coexpression in osteoblasts of broadly expressed genes accounts for the spatial restriction of ECM mineralization to bone. Genes Dev. 2005; 19:1093-1104.
21. Zhang C, Cho K, Huang Y, Lyons JP, Zhou X, Sinha K, McCrea PD, de Crombrugghe B. Inhibition of Wnt signaling by the osteoblast-specific transcription factor Osterix. Proc Natl Acad Sci U S A. 2008; 105:6936-6941.
22. Boyle WJ, Simonet WS, Lacey DL. Osteoclast differentiation and activation. Nature. 2003; 423:337-342.
23. Diascro DD, Jr., Vogel RL, Johnson TE, Witherup KM, Pitzenberger SM, Rutledge SJ, Prescott DJ, Rodan GA, Schmidt A. High fatty acid content in rabbit serum is responsible for the differentiation of osteoblasts into adipocyte-like cells. J Bone Miner Res. 1998; 13:96-106.
24. Parhami F, Morrow AD, Balucan J, Leitinger N, Watson AD, Tintut Y, Berliner JA, Demer LL. Lipid oxidation products have opposite effects on calcifying vascular cell and bone cell differentiation. A possible explanation for the paradox of arterial calcification in osteoporotic patients. Arterioscler Thromb Vasc Biol. 1997; 17:680-687.
25. Maziere C, Salle V, Gomila C, Maziere JC. Oxidized low density lipoprotein enhanced RANKL expression in human osteoblast-like cells. Involvement of ERK, NFkappaB and NFAT. Biochim Biophys Acta. 2013; 1832:1756-1764.
26. Parhami F, Jackson SM, Tintut Y, Le V, Balucan JP, Territo M, Demer LL. Atherogenic diet and minimally oxidized low density lipoprotein inhibit osteogenic and promote adipogenic differentiation of marrow stromal cells. J Bone Miner Res. 1999; 14:2067-2078.
27. Lagace TA. PCSK9 and LDLR degradation: regulatory mechanisms in circulation and in cells. Curr Opin Lipidol. 2014; 25:387-393.
28. Niemeier A, Kassem M, Toedter K, Wendt D, Ruether W, Beisiegel U, Heeren J. Expression of LRP1 by human osteoblasts: a mechanism for the delivery of lipoproteins and vitamin K1 to bone. J Bone Miner Res. 2005; 20:283-

293.
29. Chang MK, Kramer I, Huber T, Kinzel B, Guth-Gundel S, Leupin O, Kneissel M. Disruption of Lrp4 function by genetic deletion or pharmacological blockade increases bone mass and serum sclerostin levels. Proc Natl Acad Sci U S A. 2014; 111:E5187-5195.
30. Gong Y, Slee RB, Fukai N, et al. LDL receptor-related protein 5 (LRP5) affects bone accrual and eye development. Cell. 2001; 107:513-523.
31. Joiner DM, Less KD, Van Wieren EM, Hess D, Williams BO. Heterozygosity for an inactivating mutation in low-density lipoprotein-related receptor 6 (Lrp6) increases osteoarthritis severity in mice after ligament and meniscus injury. Osteoarthritis Cartilage. 2013; 21:1576-1585.
32. Lara-Castillo N, Johnson ML. LRP receptor family member associated bone disease. Rev Endocr Metab Disord. 2015; 16:141-148.
33. Leupin O, Piters E, Halleux C, et al. Bone overgrowth-associated mutations in the LRP4 gene impair sclerostin facilitator function. J Biol Chem. 2011; 286:19489-19500.
34. Tamai K, Semenov M, Kato Y, Spokony R, Liu C, Katsuyama Y, Hess F, Saint-Jeannet JP, He X. LDL-receptor-related proteins in Wnt signal transduction. Nature. 2000; 407:530-535.
35. Xiong L, Jung JU, Guo HH, Pan JX, Sun XD, Mei L, Xiong WC. Osteoblastic Lrp4 promotes osteoclastogenesis by regulating ATP release and adenosine-A2AR signaling. J Cell Biol. 2017; 216:761-778.
36. Xiong L, Jung JU, Wu H, Xia WF, Pan JX, Shen C, Mei L, Xiong WC. Lrp4 in osteoblasts suppresses bone formation and promotes osteoclastogenesis and bone resorption. Proc Natl Acad Sci U S A. 2015; 112:3487-3492.
37. Awan Z, Alwaili K, Alshahrani A, Langsetmo L, Goltzman D, Genest J. Calcium homeostasis and skeletal integrity in individuals with familial hypercholesterolemia and aortic calcification. Clin Chem. 2010; 56:1599-1607.
38. de Munter W, Blom AB, Helsen MM, Walgreen B, van der Kraan PM, Joosten LA, van den Berg WB, van Lent PL. Cholesterol accumulation caused by low density lipoprotein receptor deficiency or a cholesterol-rich diet results in ectopic bone formation during experimental osteoarthritis. Arthritis Res Ther. 2013; 15:R178.
39. Okayasu M, Nakayachi M, Hayashida C, Ito J, Kaneda T, Masuhara M, Suda N, Sato T, Hakeda Y. Low-density lipoprotein receptor deficiency causes impaired osteoclastogenesis and increased bone mass in mice because of defect in osteoclastic cell-cell fusion. J Biol Chem. 2012; 287:19229-19241.
40. Chen X, Wang C, Zhang K, Xie Y, Ji X, Huang H, Yu X. Reduced femoral bone mass in both diet-induced and genetic hyperlipidemia mice. Bone. 2016; 93:104-112.
41. Gui Y, Duan Z, Qiu X, Tang W, Gober HJ, Li D, Wang L. Multifarious effects of 17-β-estradiol on apolipoprotein E receptors gene expression during osteoblast differentiation *in vitro*. Biosci Trends. 2016; 10:54-66.
42. Qiu X, Jin X, Shao Z, Zhao X. 17β-estradiol induces the proliferation of hematopoietic stem cells by promoting the osteogenic differentiation of mesenchymal stem cells. Tohoku J Exp Med. 2014; 233:141-148.
43. Boyden LM, Mao J, Belsky J, Mitzner L, Farhi A, Mitnick MA, Wu D, Insogna K, Lifton RP. High bone density due to a mutation in LDL-receptor-related protein 5. N Engl J Med. 2002; 346:1513-1521.
44. Little RD, Carulli JP, Del Mastro RG, et al. A mutation in the LDL receptor-related protein 5 gene results in the autosomal dominant high-bone-mass trait. Am J Hum Genet. 2002; 70:11-19.
45. Choi HY, Dieckmann M, Herz J, Niemeier A. Lrp4, a novel receptor for Dickkopf 1 and sclerostin, is expressed by osteoblasts and regulates bone growth and turnover *in vivo*. PLoS One. 2009; 4:e7930.
46. Loots GG, Kneissel M, Keller H, Baptist M, Chang J, Collette NM, Ovcharenko D, Plajzer-Frick I, Rubin EM. Genomic deletion of a long-range bone enhancer misregulates sclerostin in Van Buchem disease. Genome Res. 2005; 15:928-935.
47. Chen J, Yan H, Ren DN, Yin Y, Li Z, He Q, Wo D, Ho MS, Chen Y, Liu Z, Yang J, Liu S, Zhu W. LRP6 dimerization through its LDLR domain is required for robust canonical Wnt pathway activation. Cell Signal. 2014; 26:1068-1074.
48. Ye ZJ, Go GW, Singh R, Liu W, Keramati AR, Mani A. LRP6 protein regulates low density lipoprotein (LDL) receptor-mediated LDL uptake. J Biol Chem. 2012; 287:1335-1344.
49. Brown MS, Goldstein JL. A receptor-mediated pathway for cholesterol homeostasis. Science. 1986; 232:34-47.
50. Herz J. Deconstructing the LDL receptor--a rhapsody in pieces. Nat Struct Biol. 2001; 8:476-478.
51. Rao KN. The significance of the cholesterol biosynthetic pathway in cell growth and carcinogenesis (review). Anticancer Res. 1995; 15:309-314.
52. Chao YS, Windler EE, Chen GC, Havel RJ. Hepatic catabolism of rat and human lipoproteins in rats treated with 17 alpha-ethinyl estradiol. J Biol Chem. 1979; 254:11360-11366.
53. Kovanen PT, Brown MS, Goldstein JL. Increased binding of low density lipoprotein to liver membranes from rats treated with 17 alpha-ethinyl estradiol. J Biol Chem. 1979; 254:11367-11373.
54. Ma PT, Yamamoto T, Goldstein JL, Brown MS. Increased mRNA for low density lipoprotein receptor in livers of rabbits treated with 17 alpha-ethinyl estradiol. Proc Natl Acad Sci U S A. 1986; 83:792-796.
55. Smith PM, Cowan A, White BA. The low-density lipoprotein receptor is regulated by estrogen and forms a functional complex with the estrogen-regulated protein ezrin in pituitary GH3 somatolactotropes. Endocrinology. 2004; 145:3075-3083.
56. Roubtsova A, Chamberland A, Marcinkiewicz J, Essalmani R, Fazel A, Bergeron JJ, Seidah NG, Prat A. PCSK9 deficiency unmasks a sex- and tissue-specific subcellular distribution of the LDL and VLDL receptors in mice. J Lipid Res. 2015; 56:2133-2142.

(Received October 18, 2017; Revised December 7, 2017; Accepted December 14, 2017)